

**Disalignment transitions in cold collisions of  $^3P$  atoms with structureless targets in a magnetic field**R. V. Krems<sup>1,2,\*</sup> and A. Dalgarno<sup>2</sup><sup>1</sup>Harvard-MIT Center for Ultracold Atoms, Department of Physics, Harvard University, Cambridge, Massachusetts 02138, USA<sup>2</sup>Institute for Theoretical Atomic, Molecular and Optical Physics, Harvard-Smithsonian Center for Astrophysics, Cambridge, Massachusetts 02138, USA

(Received 31 March 2003; published 11 July 2003)

A method for quantum-mechanical calculations of cross sections for the Zeeman transitions in collisions of  $^3P$  atoms with structureless targets in a magnetic field is presented and applied to the study of magnetic and electronic relaxation in oxygen-helium and carbon-helium collisions at cold and ultracold temperatures. The rate constants for collisionally induced transitions between Zeeman levels in ground-state oxygen have large magnitudes in a 1 T field. It is shown that magnetic fields induce the forbidden  $^3P_1 \rightarrow ^3P_0$  transition in ultracold collisions of carbon with helium. The cross section vanishes at zero energy for field-free collisions, but becomes infinitely large in a finite magnetic field, varying with velocity  $v$  and magnetic field  $B$  as  $B^2/v$ .

DOI: 10.1103/PhysRevA.68.013406

PACS number(s): 32.80.Pj, 32.60.+i

**I. INTRODUCTION**

In recent experiments, Doyle and co-workers [1–11] created cold atoms and molecules by a buffer gas loading technique. The method is based on collisional equilibration of the translational motion of atoms and molecules in a cold ( $<1$  K) buffer gas of helium and magnetic trapping of the slowed atoms or molecules. The atoms or molecules are trapped in their low-field seeking state which is the Zeeman level with the highest energy. Collisions with helium atoms may induce disalignment or relaxation from the Zeeman level leading to the release of energy and loss of the trapped species. The density of captured atoms in a magnetic trap is largest in the middle of the trap where the magnetic field is zero but the atoms are usually distributed over the trap region where the magnetic field  $B=0-2$  T. A complete analysis of the trapping efficiency requires the study of magnetic-field effects on the collisional processes.

All atoms trapped so far were in a state with zero electronic orbital momentum. The Zeeman transitions in collisions of  $S$ -state atoms with structureless targets such as helium are determined by the interaction of the spin angular momentum of the atoms with the orbital angular momentum for the collision—the spin-rotation interaction—which is very small. It has been proposed recently [12] to use the buffer gas loading technique for trapping atoms in states with nonzero electronic orbital angular momentum. The efficiency of the experiments will depend primarily on the relative rates of elastic energy transfer and Zeeman relaxation in collisions with helium. The mechanism for the Zeeman transitions in atoms with nonzero electronic orbital angular momentum will differ from that in  $S$ -state atoms.

The Zeeman transitions in a magnetic field have been studied experimentally for collisions of  $^3P$  and  $^2P$  atoms with rare gas atoms at high temperatures ( $\sim 230-380$  K) [13–22]. Several theoretical studies focused on disalignment

effects in the open-shell atoms [23–27], but these calculations did not account for magnetic fields. The experimental measurements were accompanied by model analyses based on perturbation theory [13] and a semiclassical method [28], but these approximate approaches may not be adequate at very low energies. To the best of our knowledge, no rigorous calculations have been reported for collisionally induced Zeeman transitions in open-shell  $P$  atoms in magnetic fields.

In this paper, we describe a method for accurate quantum calculations of cross sections for Zeeman and spin-orbit transitions in collisions of  $^3P_j$  atoms with structureless targets in a magnetic field. We investigate the magnetic-field dependence of elastic and inelastic energy transfer in cold  $O(^3P_{j=2,m_j=+2}) + \text{He}$  collisions. We show that the dynamics of spin-orbit transitions in ultracold collisions may be modified by the magnetic field. Thus, the  $^3P_{j=1} \rightarrow ^3P_{j=0}$  transition in  $C(^3P)$ -He collisions, forbidden to first order, becomes allowed in a magnetic field, and the threshold behavior of the cross section at zero energy is changed by the magnetic field.

The theory is described in Sec. II. Section III presents the results, and the conclusions are summarized in Sec. IV.

**II. THEORY**

The total Hamiltonian of the structureless atom (He)- $^3P$  atom (for example, oxygen or carbon) system in a magnetic field may be written (in atomic units) as

$$H = -\frac{1}{2\mu} \frac{d^2}{dR^2} + V_{\text{CF}} + V_{\text{ES}} + V_{\text{SO}} + V_{\text{B}}, \quad (1)$$

where  $R$  is the interatomic separation,  $\mu$  is the reduced mass of the colliding particles,  $V_{\text{ES}}$  is the nonrelativistic part of the electronic Hamiltonian,  $V_{\text{SO}}$  is the spin-orbit interaction operator,  $V_{\text{CF}}$  is the operator of the centrifugal interaction, and  $V_{\text{B}}$  is the operator describing the interaction of the open-shell  $^3P$  atom with the magnetic field.

The  $V_{\text{CF}}$  operator is given by

\*Mailing address: ITAMP, Harvard-Smithsonian CfA, 60 Garden Street, Cambridge, MA 02138, USA; electronic address: rkrems@cfa.harvard.edu

$$V_{\text{CF}} = \frac{\hat{l}^2}{2\mu R^2}, \quad (2)$$

where  $l$  is the rotational angular momentum of the  $\hat{R}$  vector joining the two atoms and is equivalent to the orbital angular momentum for collision [29]. The spin-orbit operator is represented by the scalar product of the electronic orbital angular momentum  $\hat{L}$  and the electronic spin angular momentum  $\hat{S}$ :

$$V_{\text{SO}} = A\hat{L} \cdot \hat{S}, \quad (3)$$

with a constant  $A$  related to the spin-orbit splitting.

The operator for the interaction of the  $^3P$  atom with a magnetic field has the form [30]

$$V_{\text{B}} = \mu_0(\hat{L} + 2\hat{S}) \cdot \hat{B}, \quad (4)$$

where  $\mu_0$  is the Bohr magneton and the vector  $\hat{B}$  is the magnetic field.

The vector sum of  $\hat{L}$  and  $\hat{S}$  yields the total electronic angular momentum  $\hat{j}$ . The total wave function is expanded in products of eigenfunctions of  $\hat{j}^2$  and  $\hat{l}^2$  as follows:

$$\psi = \sum_{l m_l j m_j} F_{l m_l j m_j}(R) Y_{l m_l}(\hat{R}) Y_{j m_j}(\hat{r}). \quad (5)$$

Vector  $\hat{r}$  denotes collectively the position vectors of the  $p$  electrons in the open-shell atom, and the projections of  $\hat{l}$  and  $\hat{j}$  on a space-fixed quantization axis are denoted by  $m_l$  and  $m_j$ , respectively.

The elements of the  $V_{\text{CF}}$  matrix in the basis (5) are

$$\langle l m_l j m_j | V_{\text{CF}} | j' m'_j l' m'_l \rangle = \delta_{l l'} \delta_{m_l m'_l} \delta_{j j'} \delta_{m_j m'_j} \frac{l(l+1)}{2\mu R^2}. \quad (6)$$

The spin-orbit operator is diagonal in the  $|j m_j l m_l\rangle$  representation and has the elements

$$\langle l m_l j m_j | V_{\text{SO}} | j' m'_j l' m'_l \rangle = \delta_{l l'} \delta_{m_l m'_l} \delta_{j j'} \delta_{m_j m'_j} \Delta_j, \quad (7)$$

where  $\Delta_j$  is the energy of the  $^3P_j$  atom without the magnetic field.

If the He- $^3P$  atom interaction potential is expanded in a Legendre series [31,32],

$$V_{\text{ES}}(\hat{R}) = \sum_{\lambda=0,2} \frac{4\pi}{2\lambda+1} V_{\lambda}(R) \sum_{m_{\lambda}} Y_{\lambda m_{\lambda}}^*(\hat{R}) Y_{\lambda m_{\lambda}}(\hat{r}), \quad (8)$$

the matrix elements of the  $V_{\text{ES}}$  operator in the  $|j m_j l m_l\rangle$  basis can be readily evaluated using the Wigner-Eckart theorem [33]. They have the form

$$\begin{aligned} & \langle l m_l j(LS) m_j | V_{\text{ES}} | j'(LS) m'_j l' m'_l \rangle \\ &= \sum_{\lambda=0,2} V_{\lambda} \sum_{m_{\lambda}} (-1)^{S+j+j'+\lambda+m_{\lambda}-m_l-m_j} \\ & \quad \times [(2L+1)(2L+1)(2j+1)(2j'+1)] \\ & \quad \times (2l+1)(2l'+1)]^{1/2} \begin{Bmatrix} L & j & S \\ j' & L & \lambda \end{Bmatrix} \\ & \quad \times \begin{pmatrix} j & \lambda & j' \\ -m_j & m_{\lambda} & m'_j \end{pmatrix} \begin{pmatrix} l & \lambda & l' \\ -m_l & -m_{\lambda} & m'_l \end{pmatrix} \\ & \quad \times \begin{pmatrix} L & \lambda & L \\ 0 & 0 & 0 \end{pmatrix} \begin{pmatrix} l & \lambda & l' \\ 0 & 0 & 0 \end{pmatrix}, \quad (9) \end{aligned}$$

where symbols in parentheses and curly braces are  $3j$  and  $6j$  symbols. Terms  $V_{\lambda=0}$  and  $V_{\lambda=2}$  in this equation are related to the nonrelativistic interaction potentials of the HeO or HeC molecule in the  $\Sigma$  and  $\Pi$  states as follows [34–37]:

$$\begin{aligned} V_{\lambda=0} &= (V_{\Sigma} + 2V_{\Pi})/3, \\ V_{\lambda=2} &= 5(V_{\Sigma} - V_{\Pi})/3. \end{aligned} \quad (10)$$

The quantization  $z$  axis is chosen in the direction of  $\hat{B}$ . The  $V_{\text{B}}$  operator can then be rewritten as

$$V_{\text{B}} = \mu_0 B (L_z + 2S_z), \quad (11)$$

and the elements of the  $V_{\text{B}}$  matrix can be evaluated in the basis of eigenfunctions of  $\hat{L}^2$ ,  $L_z$ ,  $\hat{S}^2$  and  $S_z$ . These functions are related to the eigenfunctions of  $\hat{j}^2$  and  $j_z$  by the transformation

$$|j m_j\rangle = \sum_{M_L M_S} \begin{bmatrix} L & S & j \\ M_L & M_S & m_j \end{bmatrix} |L M_L S M_S\rangle, \quad (12)$$

where  $M_L$  and  $M_S$  are the projections of  $\hat{L}$  and  $\hat{S}$  on the  $\hat{B}$  axis, and the symbols in the square brackets are the Clebsch-Gordan coefficients. A combination of Eqs. (11) and (12) gives the  $V_{\text{B}}$  matrix in the  $|j m_j\rangle$  representation (Table I). The  $V_{\text{B}}$  operator is diagonal in the  $l$  and  $m_l$  quantum numbers.

The  $V_{\text{B}}$  matrix is diagonal in  $m_j$  but nondiagonal in  $j$ . Thus,  $j$  is not a good quantum number. The projection of the electronic angular momentum  $m_j$  is a good quantum number asymptotically at  $R = \infty$ . The  $V_{\text{ES}}$  operator mixes different  $m_j$  states at finite interatomic separations. It follows from Eq. (9) that the matrix elements of the  $V_{\text{ES}}$  operator that couple the states with  $m_j$  and  $m_j \pm \Delta m_j$  must also couple the states with  $m_l$  and  $m_l \mp \Delta m_j$ , and there are no couplings between the states corresponding to different values of  $m_j + m_l$ . The sum  $M = m_j + m_l$  is, therefore, conserved in a collision.

For each value of the magnetic field, we define the transformation  $\mathbf{C}$  that diagonalizes the matrix of the  $V_{\text{SO}} + V_{\text{B}}$  operator. For a finite  $B$ , this transformation lifts the degen-

TABLE I. The nonzero elements of the  $V_B$  matrix for the O-He system.

$(jm_j)/(j'm'_j)$	2-2	2-1	20	21	22	1-1	10	11	00
2-2	$-3\mu_0 B$								
2-1		$-3B\mu_0/2$				$-B\mu_0/2$			
20							$-B\mu_0/\sqrt{3}$		
21				$3B\mu_0/2$				$-B\mu_0/2$	
22					$3B\mu_0$				
1-1		$-B\mu_0/2$				$-3B\mu_0/2$			
10			$-B\mu_0/\sqrt{3}$						$-\sqrt{2}B\mu_0/\sqrt{3}$
11				$-B\mu_0/2$				$3B\mu_0/2$	
00							$-\sqrt{2}\mu_0 B/\sqrt{3}$		

eracy of different  $m_j$  states corresponding to the same  $j$ , but does not mix different  $lm_l$ -states. The new channels are labeled by the quantum numbers  $l, m_l, m_j$ , and a new quantum number  $n$  in place of  $j$ . States  $|nm_j\rangle$  and  $|n'm'_j\rangle$  have different energies. The splitting of the energy levels of oxygen in the  $^3P_{j=2}$  state due to the magnetic field is illustrated in Fig. 1.

The scattering  $S$  matrix is obtained from the solution of the following system of equations:

$$\left[ \frac{d^2}{dR^2} + k_{nm_j}^2 - \frac{l(l+1)}{R^2} \right] F_{nlm_j m_j}(R) = 2\mu \sum_{n'l'm'_j} \langle nlm_j | U | n'l'm'_j \rangle F_{n'l'm'_j m'_j}(R), \quad (13)$$

where  $k_{nm_j}^2 = 2\mu(E - \epsilon_{nm_j})$ ,  $E$  is the total energy,  $\epsilon_{nm_j}$  are the eigenenergies of the  $V_{SO} + V_B$  matrix, and the elements of the coupling matrix  $\langle nlm_j | U | n'l'm'_j \rangle$  are given by

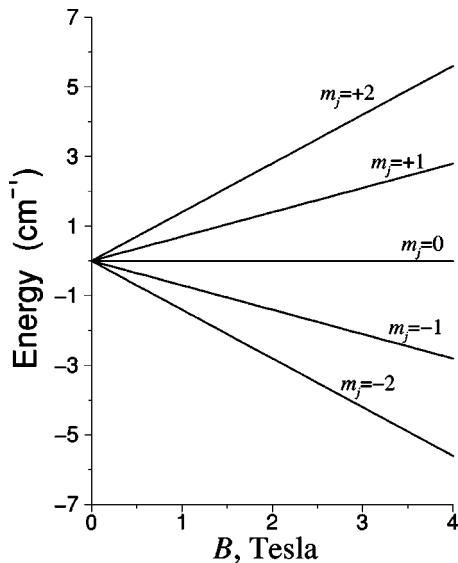


FIG. 1. Magnetic dependence of the energy levels of oxygen correlating with the  $^3P_{j=2}$  level at zero magnetic field.

$$U = C_T V_{ES} C. \quad (14)$$

The coupling matrix  $U$  is constructed for all possible values of  $M$ , and Eqs. (13) are integrated using the log-derivative propagator of Johnson and Manolopoulos [38] subject to the boundary conditions

$$F_{n'l'm'_j m'_j}^{nlm_j m_j}(R \rightarrow 0) = 0,$$

$$F_{n'l'm'_j m'_j}^{nlm_j m_j}(R \rightarrow \infty) = \frac{1}{k_{n'l'm'_j}^{1/2}} \{ \delta_{nn'} \delta_{ll'} \delta_{m_l m'_l} \delta_{m_j m'_j} \times \exp[-i(k_{nm_j} R - \pi l/2)] - S_{n'l'm'_j m'_j; nlm_j}^M \exp[i(k_{n'l'm'_j} R - \pi l'/2)] \}. \quad (15)$$

The cross sections for elastic and inelastic scattering are computed from the  $S$  matrix as follows:

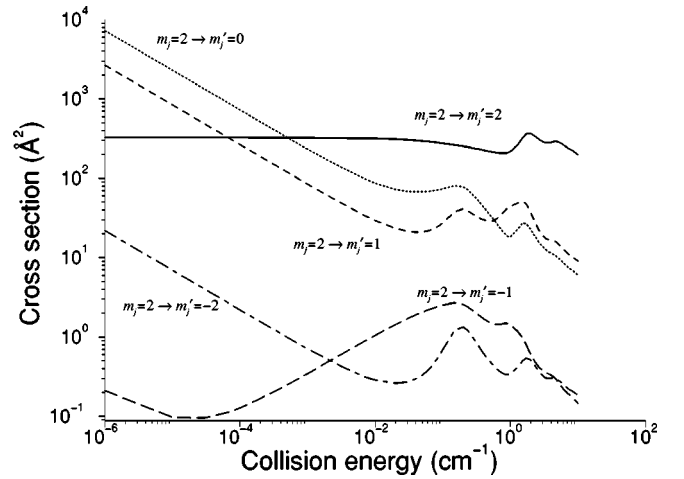


FIG. 2. Cross sections for the  $m_j = +2 \rightarrow m'_j = +2$  (full curve),  $m_j = +2 \rightarrow m'_j = +1$  (short-dashed curve),  $m_j = +2 \rightarrow m'_j = 0$  (dotted curve),  $m_j = +2 \rightarrow m'_j = -1$  (long-dashed curve), and  $m_j = +2 \rightarrow m'_j = -2$  (dot-dashed curve) transitions in  $O(^3P_{m_j=2})$ - $^3\text{He}$  collisions in the magnetic field  $B = 1$  T.

TABLE II. Rate constants ( $\text{cm}^3 \text{sec}^{-1}$ ) at temperatures of 1 and 0.5 K for the  $m_j = +2 \rightarrow m'_j$  transitions in  $\text{O}(^3P_{m_j=2})\text{-}^3\text{He}$  collisions in the magnetic field  $B=1$ .

$m'_j = +2$	$m'_j = +1$	$m'_j = 0$	$m'_j = -1$	$m'_j = -2$
			$T=1 \text{ K}$	
$0.247 \times 10^{-9}$	$0.336 \times 10^{-10}$	$0.248 \times 10^{-10}$	$0.108 \times 10^{-11}$	$0.436 \times 10^{-12}$
			$T=0.5 \text{ K}$	
$0.155 \times 10^{-9}$	$0.236 \times 10^{-10}$	$0.248 \times 10^{-10}$	$0.106 \times 10^{-11}$	$0.379 \times 10^{-12}$

$$\sigma_{nm_j \rightarrow n'm'_j} = \frac{\pi}{k_{nm_j}^2} \sum_l \sum_{m_l} \sum_{l'} \sum_{m'_l} \sum_M |\delta_{ll'} \delta_{m_l m'_l} \delta_{nn'} \delta_{m_j m'_j} - S_{nm_j l m_l; n' m'_j l' m'_l}^M|^2, \quad (16)$$

where  $S_{nm_j l m_l; n' m'_j l' m'_l}^M$  is the element of the  $S$  matrix or the probability amplitude for the  $|nm_j l m_l\rangle \rightarrow |n' m'_j l' m'_l\rangle$  transition computed at a fixed value of  $M$ .

An alternative, and somewhat more efficient, procedure is to integrate the scattering equations directly in the basis  $|lm_j m_j\rangle$  with the coupling matrix given by the sum

$$U = V_{\text{ES}} + V_{\text{B}} \quad (17)$$

and the wave numbers defined as  $k_{j m_j}^2 = 2\mu(E - \Delta_j)$ . The asymptotic log-derivative matrix must then be transformed by the  $C$  matrix as in Eq. (14) before construction of the  $S$  matrix. Both approaches give identical results.

The calculations reported in the following section were carried out with accurate interaction potentials for  $\text{He-O}(^3P)$  [39] and  $\text{He-C}(^3P)$  [40].

### III. RESULTS

#### A. Zeeman transitions in the ground-state oxygen

The magnetic  $m_j$  levels of oxygen in the  $^3P_{j=2}$  state are split in a magnetic field as shown in Fig. 1. The  $m_j = 2$  level has the highest energy and the  $\text{O}(^3P_{m_j=2})$  atoms can be captured in a magnetic trap. For the capture rate to be efficient, it is necessary that the probability for the elastic  $\text{O}(^3P_{m_j=2})\text{-He}$  collisions that cool the oxygen atoms to low temperatures be much larger than the probability of inelastic collisions leading to relaxation of the  $m_j = 2$  level.

Figure 2 shows the cross sections for elastic and  $m_j = 2 \rightarrow m'_j < 2$  inelastic collisions of oxygen with  $^3\text{He}$  in a magnetic field  $B = 1$  T and at kinetic energies  $E_{\text{col}}$  in the interval between  $10^{-6}$  and  $30 \text{ cm}^{-1}$ . The cross sections for the inelastic transitions increase as  $1/\sqrt{E_{\text{col}}}$  in the limit of low collision energies, and the elastic cross section tends to a constant value. The elastic cross section is larger than the cross sections for the  $m_j = 2 \rightarrow m'_j = 1$  and  $m_j = 2 \rightarrow m'_j = 0$  transitions at collision energies  $\geq 10^{-3} \text{ cm}^{-1}$ . Table II lists the rate constants obtained by the Boltzmann averaging of the cross sections in Fig. 2. The rate constant for the elastic energy transfer at  $T = 1$  K is only one order of magnitude larger than the rate constants for the  $m_j = 2 \rightarrow m'_j = 1$  and

$m_j = 2 \rightarrow m'_j = 0$  transitions. This indicates that, although, in principle, the buffer gas loading of oxygen atoms in a magnetic trap should be possible, it will be quite inefficient [41].

The cross section for the  $m_j = 2 \rightarrow m'_j = 0$  transition is larger than the cross section for the  $m_j = 2 \rightarrow m'_j = 1$  transition at ultralow collision energies (Fig. 2). Similarly, the probability of the  $m_j = 2 \rightarrow m'_j = -2$  transition is much larger than the probability of the  $m_j = 2 \rightarrow m'_j = -1$  transition when  $E_{\text{col}}$  is very small. We have shown earlier [42] that for odd integers  $s$ , the transitions with  $\Delta m_j = s$  and  $\Delta m_j = s + 1$  are determined by the scattering of the same partial waves. The  $\Delta m_j = s$  and  $\Delta m_j = s + 1$  transitions follow the same threshold law, and the  $\Delta m_j = s$  transitions are more efficient in  $\text{He-O}(^3P_{j=2})$  collisions than the  $\Delta m_j = s + 1$  transitions, when the  $m_j$  levels are degenerate [42]. Volpi and Bohn [43] suggested a model for the magnetic dependence of ultracold

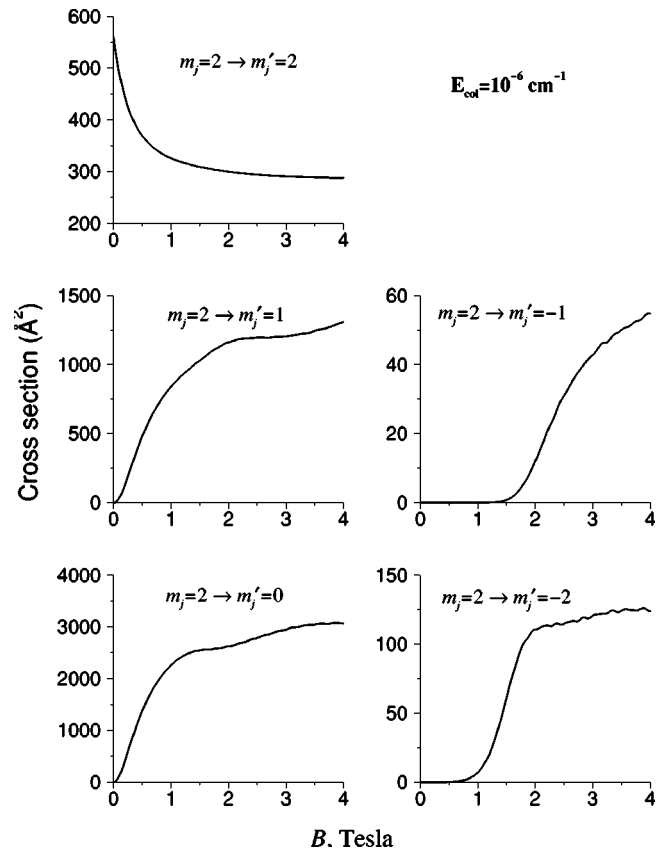


FIG. 3. Cross sections for the  $m_j = +2 \rightarrow m'_j$  transitions in  $\text{O}(^3P_{m_j=2})\text{-}^3\text{He}$  collisions as functions of the magnetic-field strength  $B$  at a collision energy of  $10^{-6} \text{ cm}^{-1}$ .

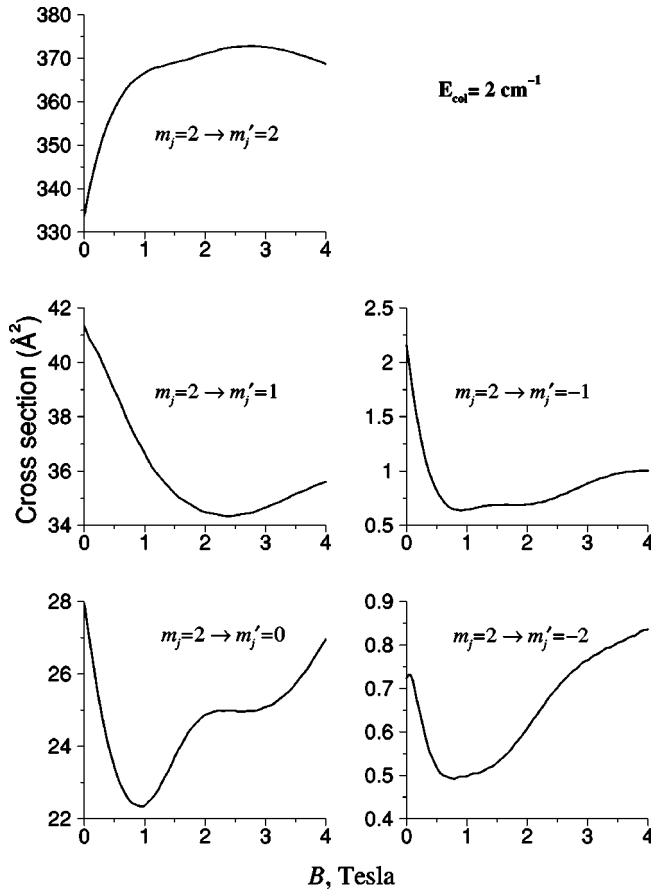


FIG. 4. Cross sections for the  $m_j = +2 \rightarrow m'_j$  transitions in  $O(^3P_{m_j=2})\text{-}^3\text{He}$  scattering at a collision energy of  $2 \text{ cm}^{-1}$  as functions of the magnetic-field strength  $B$ .

inelastic atom-molecule collisions which can be used to explain the anomalous ratio of the  $\Delta m_j = s + 1$  to  $\Delta m_j = s$  cross sections in a magnetic field. When the energy defect between the initial and the final scattering states is small and the collision energy is low, the height of the centrifugal barrier in the final state can be larger than the initial energy of the system and the inelastic collision is suppressed by the centrifugal maximum in the outgoing channel. Increasing the energy gap between the initial and the final states should increase the probability of escaping the barrier. Volpi and Bohn [43] proposed a semiempirical formula which indicates that the cross sections for the Zeeman transitions at ultracold temperatures increase with magnetic field strength. Figure 3 shows the magnetic-field dependence of cross sections for  $m_j = 2 \rightarrow m'_j$  transitions in oxygen at an ultralow collision energy. Although the formula of Bohn and Volpi predicts a monotonic increase of the transition probabilities with  $B$ , our data show that the initial rapid increase of the cross section levels off at high values of  $B$ . When  $B$  is high, the splitting of the  $m_j$  levels is so large that the centrifugal barrier in the final channel does not affect the cross section and the arguments of Volpi and Bohn do not apply. The suppression and enhancement of spin-flip transitions due to the centrifugal barrier in the final scattering state have also been observed

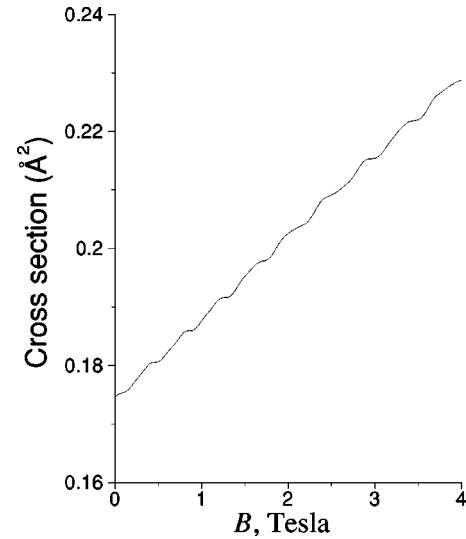


FIG. 5. Cross section for the  $m_j = 2 \rightarrow m'_j = -2$  transition in  $O(^3P)\text{-}^3\text{He}$  collisions at a collision energy  $10 \text{ cm}^{-1}$  as a function of the magnetic-field strength.

by Zygelman and Dalgarno in Na-Na ultracold collisions [44].

Figure 4 shows the magnetic-field dependence of cross sections for  $m_j$  transitions at a collision energy comparable with the energy difference between the Zeeman levels. The inelastic cross sections decrease as  $B$  increases from 0 to 1 T, pass through a minimum and increase with further increase of  $B$ . The initial decrease of the cross section with  $B$  is, apparently, due to the increase of the energy separation and the energy gap law. At high magnetic field, couplings between the states corresponding to different total angular momenta are enhanced and increase the total cross sections. At still higher collision energies ( $\sim 10 \text{ cm}^{-1}$ ), the effect of the energy gap is less significant and the cross sections for the  $m_j$ -changing transitions, shown in Fig. 5, increase slowly as  $B$  increases from 0 to 4 T. An increase of the cross sections for the Zeeman transitions with the magnetic-field strength at high collision energies has been observed experimentally for  $\text{Cs}(^2P_{1/2})\text{-He}$  collisions at values of  $B = 0\text{--}4 \text{ T}$  [13] and a similar explanation was given. When the magnetic field was increased beyond 4 T, the cross section for the  $m_j$ -changing transition in Cs showed a fall off. The effect has not been definitively explained [13].

### B. Forbidden $^3P_1 \rightarrow ^3P_0$ transition in a magnetic field

Because the electrostatic interaction does not couple the  $^3P_{j=1}$  and  $^3P_{j=0}$  states, the transition between them is forbidden in first order [32,45–50]. We have shown earlier [40,51] that the  $^3P_{j=1} \leftrightarrow ^3P_{j=0}$  transition cannot occur at zero temperature in collisions at  $B = 0$ . As indicated in Table I, however, the interaction with the magnetic fields would couple the states and the  $^3P_{j=1} \rightarrow ^3P_{j=0}$  transition becomes allowed. Figure 6 shows the energy levels of carbon, split by the magnetic field.

Figure 7 shows cross sections for the transition from the  $m_j = 1$  state correlating with the  $^3P_{j=1}$  level to the  $m_j = 0$

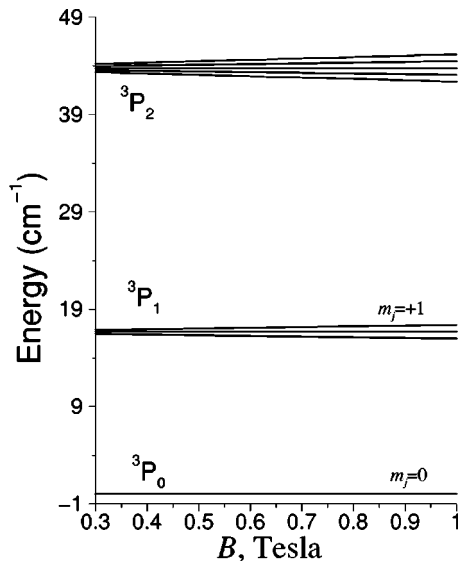


FIG. 6. Magnetic dependence of the energy levels of carbon correlating with the  ${}^3P_{j=2}$ ,  ${}^3P_{j=1}$ , and  ${}^3P_{j=0}$  levels at zero magnetic field.

state correlating with the  ${}^3P_{j=0}$  level in carbon-helium collisions at different magnetic field strengths. In the presence of a magnetic field, the cross section passes through a minimum at some low energy and then rises to infinity inversely as the velocity to yield a finite rate coefficient at zero temperature. In the limit of zero collision energy, the rate coefficient varies as the square of the magnetic field.

#### IV. SUMMARY

We have developed a methodology for quantum time-independent calculations of cross sections for Zeeman and spin-orbit transitions in a magnetic field and have applied it to the study of magnetic and electronic relaxation in cold collisions of  $O({}^3P)$  and  $C({}^3P)$  with helium. We have concluded that the Zeeman transitions are induced by interaction of the electronic orbital angular momentum  $L$  and the rotational angular momentum of the diatom  $l$ . This interaction is strong and the  $\Delta m_j = 1$  and 2 transitions in  $O({}^3P_{m_j=2})$ -He collisions are only one order of magnitude slower than the elastic energy transfer at low temperatures. We have found that the variation of cross sections for the Zeeman transitions

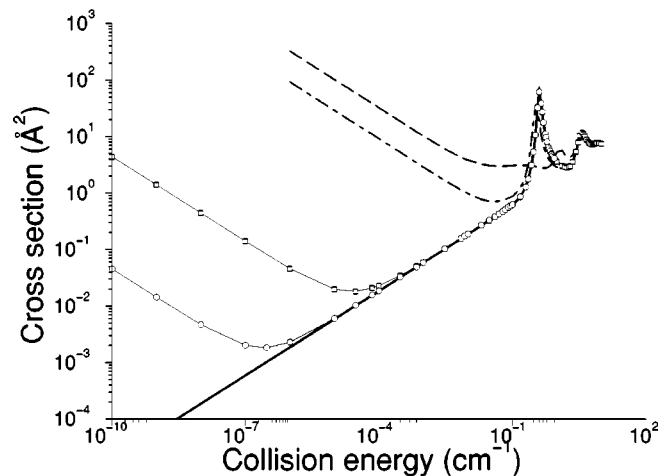


FIG. 7. Cross sections for the  $m_j = 1 \rightarrow m_j' = 0$  electronic transition (the transition between the states labeled in Fig. 6): full curve  $-B = 0$ , curve with circles  $-B = 10^{-4}$  T, curve with squares  $-B = 10^{-3}$  T, dot-dashed curve  $-B = 0.1$  T, and broken curve  $-B = 1$  T.

in oxygen with magnetic field is not significant except for ultralow collision energies where the outcome of a collision is determined by centrifugal barriers in the final scattering channels or at energies near scattering resonances. We have demonstrated that magnetic fields may couple the electronic states which would otherwise be uncoupled, thereby changing the dynamics of electronic transitions. Thus, the cross section for the transition from the  $m_j = 1$  state correlating with the  ${}^3P_{j=1}$  level to the  $m_j = 0$  state correlating with the  ${}^3P_{j=0}$  level in carbon-helium collisions varies as  $B^2/\sqrt{E_{\text{col}}}$  and changes from zero to infinity at zero collision energy, when a magnetic field is applied.

#### ACKNOWLEDGMENTS

We thank John Doyle for stimulating this work. The research was supported by the Center for Ultracold Atoms at Harvard University and Massachusetts Institute of Technology and the Institute for Theoretical Atomic, Molecular and Optical Physics at the Harvard-Smithsonian Center for Astrophysics. The work of A.D. was supported by a grant from Chemical Sciences, Geosciences and Biosciences Division of the Office of Basic Energy Sciences, Office of Science, U.S. Department of Energy.

- [1] J.M. Doyle, B. Friedrich, J. Kim, and D. Patterson, Phys. Rev. A **52**, R2515 (1995).
- [2] J. Kim, B. Friedrich, D.P. Katz, D. Patterson, J.D. Weinstein, R. DeCarvalho, and J.M. Doyle, Phys. Rev. Lett. **78**, 3665 (1997).
- [3] J.D. Weinstein, R. DeCarvalho, J. Kim, D. Patterson, B. Friedrich, and J.M. Doyle, Phys. Rev. A **57**, R3173 (1998).
- [4] J.D. Weinstein, R. DeCarvalho, K. Amar, A. Boca, B.C. Odom, B. Friedrich, and J.M. Doyle, J. Chem. Phys. **109**, 2656 (1998).
- [5] J.D. Weinstein, R. DeCarvalho, T. Guillet, B. Friedrich, and

J.M. Doyle, Nature (London) **395**, 148 (1998).

- [6] B. Friedrich, J.D. Weinstein, R. DeCarvalho, and J.M. Doyle, J. Chem. Phys. **110**, 2376 (1999).
- [7] R. DeCarvalho, J.M. Doyle, B. Friedrich, T. Guillet, J. Kim, D. Patterson, and J.D. Weinstein, Eur. Phys. J. D **7**, 289 (1999).
- [8] D. Egorov, J.D. Weinstein, D. Patterson, B. Friedrich, and J.M. Doyle, Phys. Rev. A **63**, 030501 (2001).
- [9] J.D. Weinstein, R. DeCarvalho, C.I. Hancox, and J.M. Doyle, Phys. Rev. A **65**, 021604 (2002).
- [10] J. Kim, Ph.D. thesis, Harvard University, 1997.
- [11] J.D. Weinstein, Ph.D. thesis, Harvard University, 2002.

- [12] C. Hancox and J.M. Doyle (private communication).
- [13] W. Kedzierski, J. Gao, W.E. Baylis, and L. Krause, *Phys. Rev. A* **49**, 4540 (1994).
- [14] M.D. Rotondaro and G.P. Perram, *Phys. Rev. A* **58**, 2023 (1998).
- [15] J. Luo, Z. Wu, M. Zhao, A. Chen, and X. Zeng, *J. Phys. B* **29**, 3319 (1996).
- [16] S. Matsumoto, K.I. Shiozawa, Y. Ishitani, A. Hirabayashi, and T. Fujimoto, *Phys. Rev. A* **44**, 4316 (1991).
- [17] J.C. Gay and W.B. Schneier, *Phys. Rev. A* **20**, 894 (1979).
- [18] J.C. Gay and W.B. Schneider, *Phys. Rev. A* **20**, 905 (1979).
- [19] J.C. Gay and A. Omont, *J. Phys. (Paris)* **37**, L69 (1976).
- [20] W. Berdowski and L. Krause, *Phys. Rev.* **165**, 158 (1968).
- [21] B. Niewitecka and L. Krause, *Phys. Rev. A* **12**, 2407 (1975).
- [22] R. Boggy and F.A. Franz, *Phys. Rev. A* **25**, 1887 (1982).
- [23] M. Kimura, H. Kato, K. Someda, and H. Nakamura, *J. Chem. Phys.* **96**, 7423 (1992).
- [24] C. Bahrim, H. Kucal, and F. Masnou-Seeuws, *Phys. Rev. A* **56**, 1305 (1997).
- [25] C. Bahrim, H. Kucal, O. Dulieu, and F. Masnou-Seeuws, *J. Phys. B* **30**, L797 (1997).
- [26] L.J. Kovalenko, S.R. Leone, and J.B. Delos, *J. Chem. Phys.* **91**, 6948 (1989).
- [27] G.C. Schatz, L.J. Kovalenko, and S.R. Leone, *J. Chem. Phys.* **91**, 6961 (1989).
- [28] J.C. Gay and W.B. Schneider, *Phys. Rev. A* **20**, 879 (1979).
- [29] The caret over symbols denotes vectors and nonscalar operators. The notations  $Y(\hat{R})$  and  $Y(\hat{r})$  assume that the spherical harmonics  $Y$  depends on the orientation of the vectors  $\hat{R}$  and  $\hat{r}$ , respectively.
- [30] L.D. Landau and E.M. Lifshitz, *Quantum Mechanics* (Gos. Izd., Moscow, 1963).
- [31] J. Callaway and E. Bauer, *Phys. Rev.* **140**, A1072 (1965).
- [32] R.H.G. Reid and A. Dalgarno, *Phys. Rev. Lett.* **22**, 1029 (1969).
- [33] R.N. Zare, *Angular Momentum* (Wiley, New York, 1988).
- [34] V. Aquilanti, R. Candori, and F. Pirani, *J. Chem. Phys.* **89**, 6157 (1988).
- [35] V. Aquilanti, D. Cappelletti, V. Lorent, E. Luzzatti, and F. Pirani, *J. Phys. Chem.* **89**, 2063 (1992).
- [36] V. Aquilanti, D. Cappelletti, V. Lorent, E. Luzzatti, and F. Pirani, *Chem. Phys. Lett.* **192**, 153 (1992).
- [37] V. Aquilanti and G. Grossi, *J. Chem. Phys.* **73**, 1165 (1980).
- [38] B.J. Johnson, *J. Comput. Phys.* **13**, 445 (1973); D.E. Manolopoulos, *J. Chem. Phys.* **85**, 6425 (1986).
- [39] R.V. Krems, A.A. Buchachenko, M.M. Szczesniak, J. Klos, and G. Chalasinski, *J. Chem. Phys.* **116**, 1457 (2002).
- [40] R.V. Krems, D. Zgid, G. Chalasinski, J. Klos, and A. Dalgarno, *Phys. Rev. A* **66**, 030702 (2002).
- [41] Typically, it is required that the elastic-to-inelastic ratio be more than 100 for the buffer gas loading to work efficiently.
- [42] R.V. Krems and A. Dalgarno, *Phys. Rev. A* **67**, 050704(R) (2003).
- [43] A. Volpi and J.L. Bohn, *Phys. Rev. A* **65**, 052712 (2002).
- [44] B. Zygelman and A. Dalgarno, *J. Phys. B* **35**, L441 (2002).
- [45] M.H. Alexander, T. Orlikowski, and J.E. Straub, *Phys. Rev. A* **28**, 73 (1983).
- [46] Z. Ma, K. Liu, L.B. Harding, M. Komotos, and G.C. Schatz, *J. Chem. Phys.* **100**, 8026 (1994).
- [47] T.S. Monteiro and D.R. Flower, *Mon. Not. R. Astron. Soc.* **228**, 101 (1987).
- [48] R.H.G. Reid, *J. Phys. B* **6**, 2018 (1973).
- [49] R.H.G. Reid and A. Dalgarno, *Chem. Phys. Lett.* **6**, 85 (1970).
- [50] R.V. Krems and A.A. Buchachenko, *J. Phys. B* **33**, 4551 (2000).
- [51] R.V. Krems and A.A. Buchachenko, *Phys. Rev. A* **64**, 024704 (2001).